硅球多层模板溶胶浸渍法制备有序多孔 TiO_2 薄膜

刘国奇 靳正国* 方 宏 刘同军
(先进陶瓷与加工技术教育部重点实验室,天津大学材料学院,天津 300072)

摘要: 采用垂直沉积法组装了平均球径为 188 nm 的三维有序二氧化硅微球阵列。以该阵列为模板,通过在 TiO_2 前驱体溶胶中多次浸渍热处理循环,随后采用超声辅助的 NaOH 溶液腐蚀去除硅球模板,制备了>20 层厚的反转结构的二氧化钛多孔膜。该二氧化钛薄膜在 550 ℃下热处理 20 h 其多孔结构保持不变, 表明采用此方法制备的二氧化钛多孔膜具有较好的热稳定性。X 射线衍射图表明 550 ℃下热处理得到的是具有锐钛矿结构的二氧化钛多孔膜。透光光谱显示了光子带隙出现在~400 nm。通过 SEM 观察,二氧化钛多孔膜的平均孔径为 180 nm (±3),收缩率约为 4.3%,与布拉格衍射方程计算的结果 176 nm 有较好的吻合。

关键词: 二氧化钛多孔膜; 多层结构; 溶胶-凝胶; 硅球模板
中图分类号: O614.41; TB383 **文献标识码**: A **文章编号**: 1001-4861(2007)09-1528-05

Ordered Porous TiO_2 Films Assembled by Sol-dipping Method with Multilayer Silica Spheres Template

LIU Guo-Qi JIN Zheng-Guo* FANG Hong LIU Tong-Jun
(*Key Laboratory for Advanced Ceramics and Machining Technology of Ministry of Education, School of Materials, Tianjin University, Tianjin* 300072)

Abstract: Three-dimensionally ordered porous TiO_2 films were prepared by sol-dipping method using silica spheres multilayer templates. The templates were previously assembled on glass substrates by vertical deposition method from purified silica spheres alcosol. Ultrasonic-assisted NaOH etching was employed in the removal of silica spheres templates. The inverted TiO_2 film was heat-treated at 550 ℃ for 20 h and the porous structure remained unchanged implying a good thermal stability. X-ray diffraction (XRD) results indicate that the inverted TiO_2 film is with anatase structure. ESEM images show that the average center-to-center distance between pores of the TiO_2 film is 180 nm (±3), about 4.3% smaller than that of the original silica sphere, which is consistent with the value of 176 nm calculated according to the Bragg law. The transmission spectrum shows an attenuation band around wavelength of 400 nm.

Key words: ordered porous TiO_2 film; multilayer structure; silica sphere template; sol-gel

TiO_2 films with three-dimensionally ordered porous structure have recently attracted much attention because of their promising applications in electronic, electrochemical, and photocatalytic systems such as photoelectrochemical solar cells [1,2], electrocatalysts [3], sensors[4] and high-performance photocatalysts[5]. A number of methods have been developed for the 3D-TiO_2 fabrication, in which the template replication of colloidal crystals provides a simple and efficient method [6 ~10]. This routine usually assembles close-

收稿日期:2007-03-22。收修改稿日期:2007-07-25。
天津市基础研究重点项目(No.07JCZDJC00900)资助。
*通讯联系人。E-mail:zhgjin@tju.edu.cn
第一作者:刘国奇,男,29 岁,博士;研究方向:半导体薄膜材料的研究。

packed colloidal crystal arrays of monodisperse inorganic or organic spheres (typically silica or polystyrene) as templates by vertical deposition or gravity sedimentation method, and then fills the interstices among the close-packed arrays of silica or polystyrene spheres with a precursor, which forms a solid skeleton around the spheres. Finally, a well-defined porous material with narrow pore size distribution can be obtained when the templates are removed by either chemical etching or heat treatment.

For assembly of porous TiO_2 film, the removal of organic template was prone to cause the collapse of pore structure because the pyrolysis volatilization of organic template was prior to the crystallization of TiO_2 skeletons. However, the disadvantage could be avoided by silica speres templating method because that the supported TiO_2 skeletons remain unchanged during crystallization of the inorganic frame and is generally removed by chemical etching after annealing. In this work, an artificial silica opal with over 20 layers was used to replicate three-dimensionally ordered porous TiO_2 film by sol-dipping method. Particularly, the ultrasonic-assisted basic etching was employed for the removal of silica spheres templates, which effectively improves the etching rate of the multilayer templates with deep infiltrating path. The ordered porous TiO_2 films were characterized by ESEM, TEM, XRD, EDS and UV-Vis. The Bragg law was used to calculate the diameter of air spheres in the porous TiO_2 structure.

1 Experimental

In the preparation of silica colloidal crystals and TiO_2 sol, the following chemicals were used: tetraethoxysilane [$Si(OC_2H_5)_4$, A.R., Kermel, Tianjin], tetrabuty-lorthotitanate [$Ti(OC_4H_9)_4$, A.R., Kermel, Tianjin], dietha-nolamine [$NH(CH_2CH_2OH)_2$, A.R., Damao, Tianjin], ethanol (CH_3CH_2OH, AR, Kewei, Tianjin), ammonia ($NH_3 \cdot H_2O$, A.R., Kewei, Tianjin), deionized water (Nankai University, Tianjin) and 15% aqueous NaOH (Kewei, Tianjin) solution.

Silica spheres were synthesized by Stober-Fink-Bohn method[11], using $Si(OC_2H_5)_4$ as the starting material. Multilayer silica colloidal crystal templates were deposited onto glass microslides through a convective assembly process[12]. The resultant colloidal templates on glass microslides were sintered at 550 ℃ for 1 h to form small contact necks among silica spheres. The 0.2 $mol \cdot L^{-1}$ TiO_2 precursor sol was prepa-red at room temperature by hydrolysis of titanium tetrabutylorthotitanate in ethanol-diethanolamine-deionized water mixed solution with molar ratio of 77∶1∶1. For infiltration of TiO_2 precursor sol, the silica crystalline templates on substrates were vertically immersed into TiO_2 precursor sol in a beaker for 10 min and then slowly drawn up out of TiO_2 precursor sol. After that, it was dried at 100 ℃ for 15 min and sintered at 550 ℃ for 1 h to crystallize and densify the titania frame inside. The above infiltration cycle was repeated for 12 times in order to make enough TiO_2 padding into the interstices among the close-packed silica spheres arrays. The resulting titania-opal composite was ultrasonically immersed into 15% NaOH aqueous solution at 50 ℃ for 4 h to remove the silica template, leaving a fully porous titania structure. To explore its thermal stability, the inverted porous titania film was heat-treated at 550 ℃ for 20 h. In addition, a template-free compact TiO_2 film derived from the same TiO_2 sol-gel processing was prepared as reference for comparison with the porous film.

TEM observation of Silica spheres was performed on a JEOL 100CX-Ⅱ transmission electron microscopy (accelerating voltage 100 kV). ESEM and EDS were carried out by PHILIPS XL-30 environment scanning electron microscopy (accelerating voltage 20 kV) and Oxford INCA Energy 300 (accelerating voltage 20 kV, working distance 12 mm), respectively. X-ray diffraction (XRD) patterns were recorded with a Rigaku D/max-2500 X-ray diffractometer [Cu $K\alpha$ radiation (λ = 0.154 06 nm), graphite monochromator filter, target voltage 40 kV, current 200 mA, scanning range 10°~80°, scanning rate $6° \cdot min^{-1}$]. The optical trans-mittance spectra were detected by DU-8B UV/Vis double-beam spectrophotometer.

2 Results and discussion

Fig.1 shows the TEM image of the silica spheres

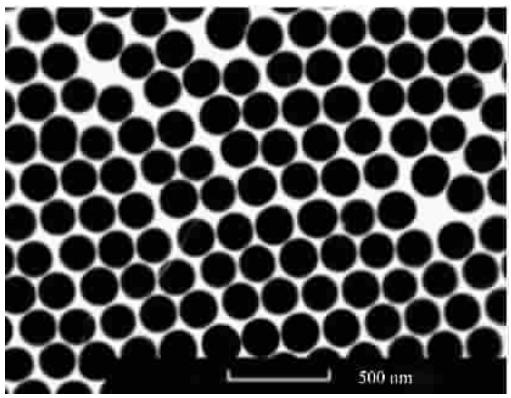

Fig.1 TEM image of silica spheres

synthesized by the Stober-Fink-Bohn method. It can be seen that the silica spheres are monodispersed and the average diameter is about 188 nm with a dispersion of smaller than 6%.

Fig.2 shows ESEM images of the silica spheres template assembled by the vertical deposition method. From Fig.2 (a), we can see that the silica spheres colloidal crystal template have hexagonal close packing structure on a larger area. Fig.2(b) is the side view of the silica spheres colloidal crystal array, displaying that the close-packed structure extends uniformly over 20 layers.

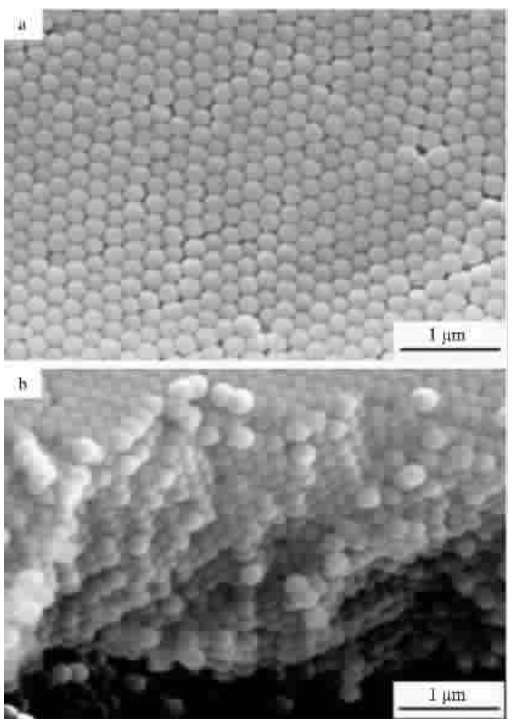

Fig.2 ESEM images of silica spheres template:
(a) top view; (b) side view

For infiltration of TiO_2 precursor sol, as known from our previous study [13], the high concentration of TiO_2 sol had poor permeation in the filling among the close-packed silica spheres. Although it is easy to infiltrate the interstices with low concentration of TiO_2 sol, there is not enough solid content in TiO_2 sol to fully fill the interstices with limited dipping cycles. In this work, TiO_2 sol with concentration of 0.2 mol·L^{-1} was used. Fig.3 shows the ESEM images of the 3D inverted porous titania film. It can be seen that the ordered close packing of the silica spheres template is clearly imprinted into the titania matrix, even in the inner layers as shown in Fig.3 (b). The direct observation by ESEM reveals that the average center-to-center distance between pores is 180 nm (±3), about 4.3% smaller than that of the original silica spheres. Fig.4 is the corresponding EDS pattern, and it shows that the atomic ratio of Si and Ti is about 1∶64 when other elements are neglected except Si, O and Ti. The ultrasonic-assisted basic etching provides an effective way for template removal as shown by the above results. However, it should be pointed out that some defects exist in the TiO_2 matrix, which needs to be improved in further study by optimization of the ultrasonic-assisted basic etching.

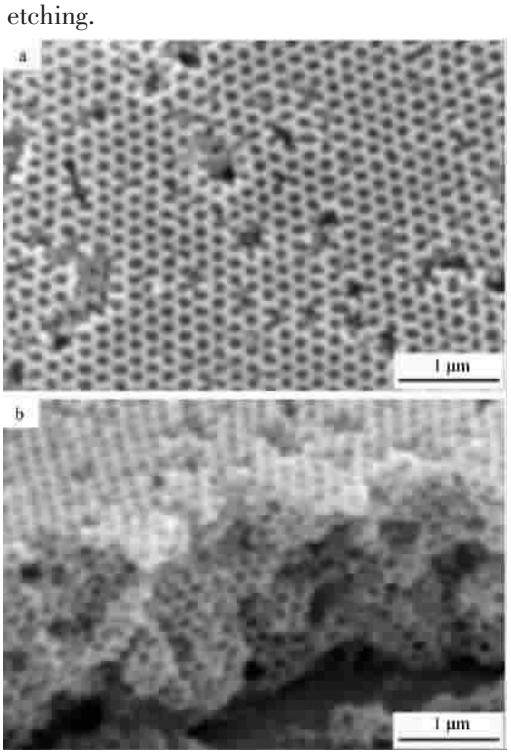

Fig.3 ESEM images of the inverted TiO_2 porous film:
(a) top view; (b) side view

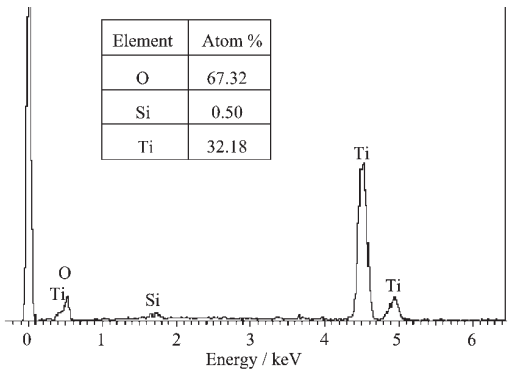

Fig.4　EDS spectrum of the inverted TiO_2 porous film

Fig.5 shows the ESEM images of the inverted TiO_2 film which was heat-treated at 550 ℃ for 20 h. It can be seen that the three-dimensional porous structure of the heat-treated TiO_2 film retains integrity, which indicates the replicated porous TiO_2 film possesses good thermal stability.

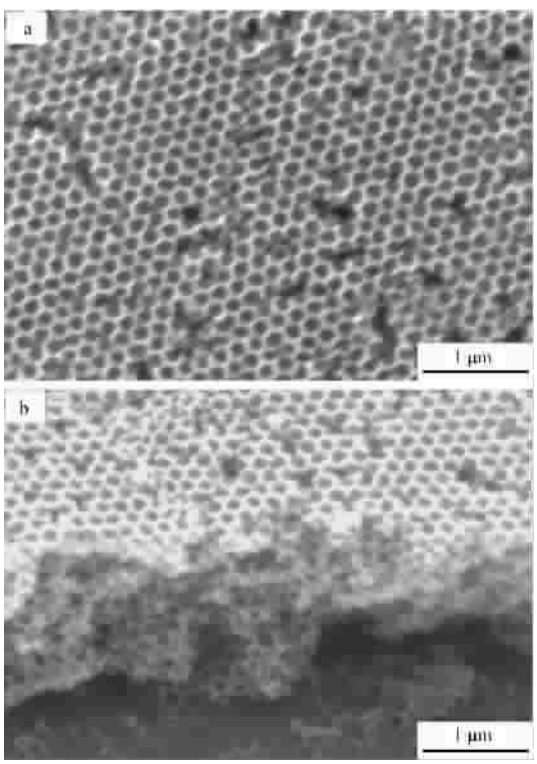

Fig.5　ESEM images of the inverted TiO_2 porous film heat-treated at 550 ℃ for 20 h: (a) top view; (b) side view

Fig.6 shows X-ray diffraction (XRD) patterns of the inverted porous TiO_2 film and compact one, both heat-treat at 550 ℃ for 1 h. For the inverted porous film, characteristic peaks can be observed at 2θ=25.3° and 47.6°, corresponding to (101), (200) reflections of anatase structure, respectively. These peaks can also be seen in the same positions for the compact TiO_2 film, suggesting that the inverted porous assembly with multilayer silica colloidal crystal template does not obviously affect the intrinsic crystallization characteristics of TiO_2 derived from the sol-gel processing. Moreover, it should be explained that the protruding background in the range of 15°~40° originates from the diffraction of glass substrates.

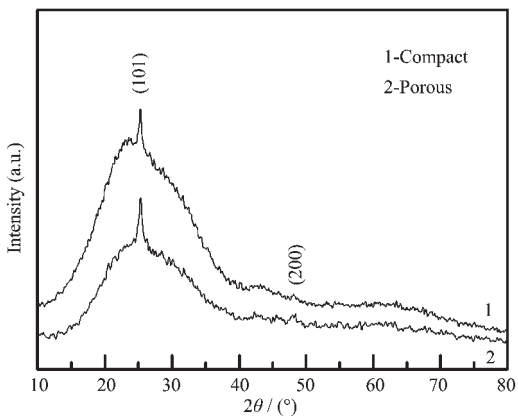

Fig.6　XRD patterns of both TiO_2 films heat-treated at 550 ℃ for 1 h

Optical transmittance of the inverted porous and compact TiO_2 films in the wavelength (λ) range of 300~900 nm is shown in Fig.7. Compared with the latter, the former presents a pronounced attenuation dip on transmission curve around 400 nm, which corresponds to coherent Bragg scattering on parallel sets of (111) planes of the porous structure. To calculate pore diameter, the following Bragg equation at normal incidence was adopted:

$$\lambda = 2n_e d_{(111)}$$

where n_e is the effective refractive index of the porous TiO_2 structure. For the anatase phase, the average value of the refractive index is 2.5. When the TiO_2 padding is assumed in the fully filling state in the voids of the template (occupying 26 vol% of unit cube), n_e is 1.39=2.5×26%+1×74% according to reference[14]. And $d_{(111)}$ is the distance between parallel lattice planes. For face-center cubic (FCC) structures, $d_{(111)}=\sqrt{2/3}\,D$, where D is pore diameter. So, the calculated value of pore diameter is 176 nm, which consists with that measured by ESEM observation.

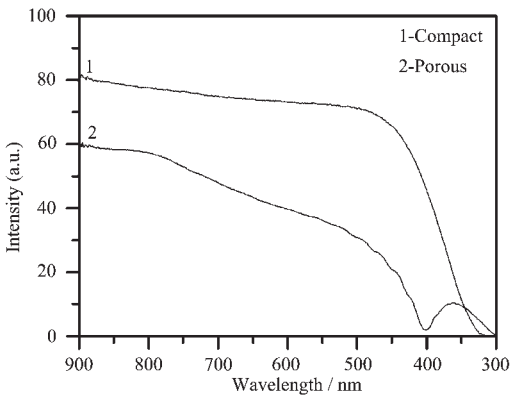

Fig.7 Optical transmittance spectra of TiO_2 films

3 Conclusions

Ordered porous TiO_2 film could be replicated by sol-dipping method using silica spheres colloidal crystals with over 20 layers. Enough TiO_2 padding into the interstices among the close-packed silica spheres is achieved through repeating the infiltration cycle 12 times, followed by annealing at 550 ℃ for 1 h each cycle. Finally, the silica spheres template with over 20 layers could be removed by ultrasonic-assisted NaOH etching. Better thermal stability of the inverted porous titania film is identified by heat-treating at 550 ℃ for holding 20 h. The pore diameter of the obtained porous TiO_2 film measured by ESEM is 180 nm, about 4.3% smaller than that of original silica spheres. The pore diameter calculated based on the Braggs law and the attenuation dip on transmission curve is 176 nm, showing a good agreement with that measured by ESEM.

References:

[1] ORegan B, Grtzel M. *Nature*, **1991**,**353**:737~740

[2] ORegan B, Schwartz D T, Zakeeruddin S M, et al. *Adv. Mater.*, **2000**,**12**(17):1263~1267

[3] Lakshmi B B, Dorhourt P K, Martin C R. *Chem. Mater.*, **1997**, **9**(3):857~862

[4] Lin H M, Hsu T Y, Tung C Y, et al. *Nanostructured Mater.*, **1995**,**6**(5~8):1001~1004

[5] Gopidas K R, Bohorques M, Kamat P V. *J. Phys. Chem.*, **1990**,**94**(16):6435~6440

[6] Wijinhoven J E G J, Vos W L. *Science*, **1998**,**281** (5378): 802~804

[7] Yan H, Blanford C F, Holland B T, et al. *Chem. Mater.*, **2000**,**12**(4):1134~1141

[8] Vlasov Y A, Bo X Z, Sturm J C, et al. *Nature*, **2001**,**414** (6861):289~293

[9] Dong W, Bongard H, Tesche B, et al. *Adv. Mater.*, **2002**,**14** (20):1457~1460

[10]Míguez H, Tétreault N, Yang S M, et al. *Adv. Mater.*, **2003**, **15**(7~8):597~600

[11]Stober W, Fink A, Bohn E. *J. Colloid Interface Sci.*, **1968**, **26**(1):62~69

[12]Jiang P, Bertone J F, Hwang K S, et al. *Chem. Mater.*, **1999**,**11**(8):2132~2140

[13]Liu Z F, Jin Z G, Liu X X, et al. *J. Sol-gel Sci. Tech.*, **2006**, **38**(1):73~78

[14]Meng Q B, Fu C H, Einaga Y, et al. *Chem. Mater.*, **2002**,**14** (1):83~88